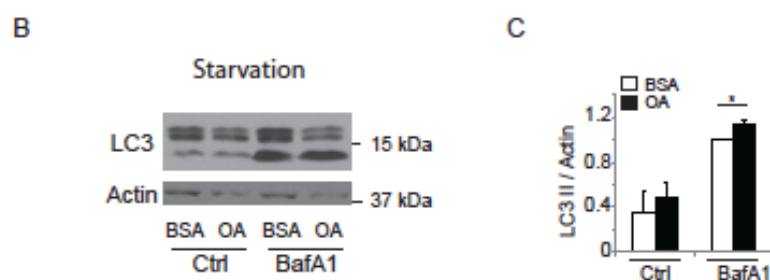
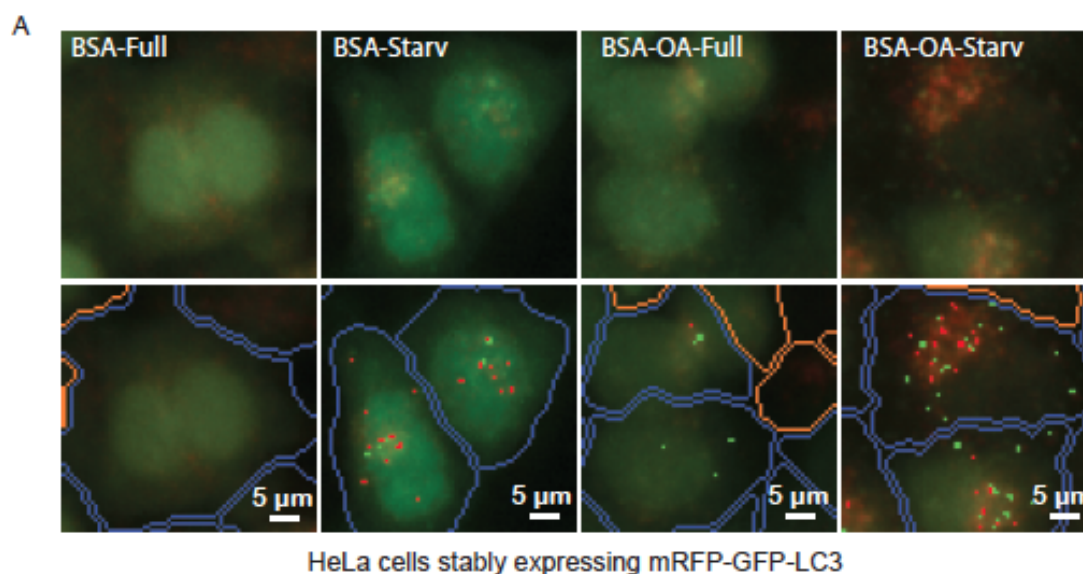
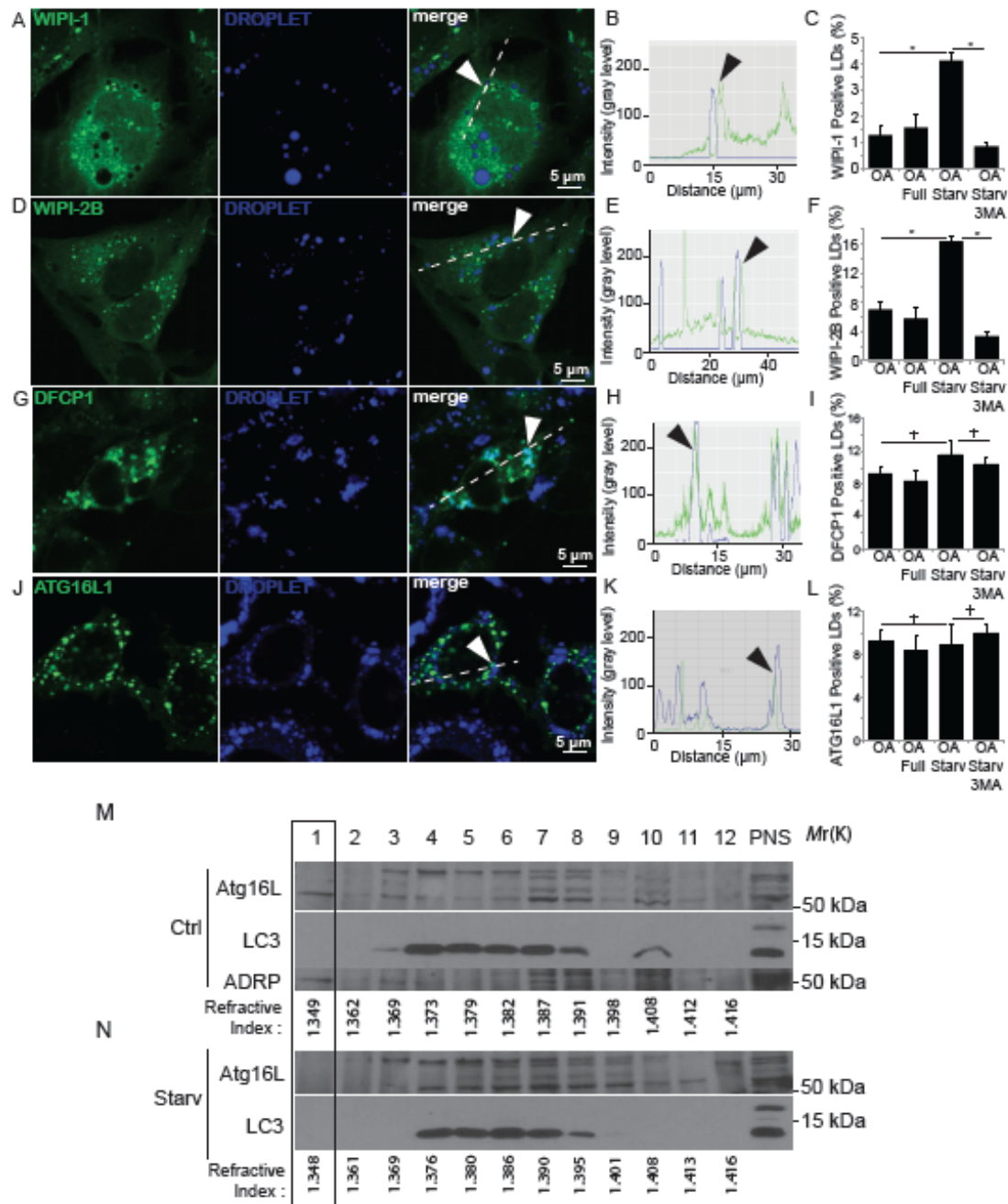


Supplemental Information



Supplementary Figure S1. Preformed lipid droplets enhance starvation-induced autophagy.

(A) Fluorescent images acquired by high content microscopy. Program-assigned masks: blue outline, valid primary objects (cells); green mask, GFP puncta. HeLa cells stably expressing mRFP-GFP-LC3 were treated for 20 h with BSA alone (BSA) or with BSA-oleic acid (OA; 500 μ M OA) and then starved in EBSS for 90 min (Starv) or incubated in full medium (Full). (B,C) HeLa cells were treated for 20 h with BSA alone or with BSA-OA (500 μ M OA), followed by starvation in EBSS for 90 min with or without Bafilomycin A1 (BafA1) and LC3-II/actin ratios determined by immunoblotting (B) and densitometry (C). Immunoblotting data: means \pm s.e., *, $p < 0.05$ (t-test).

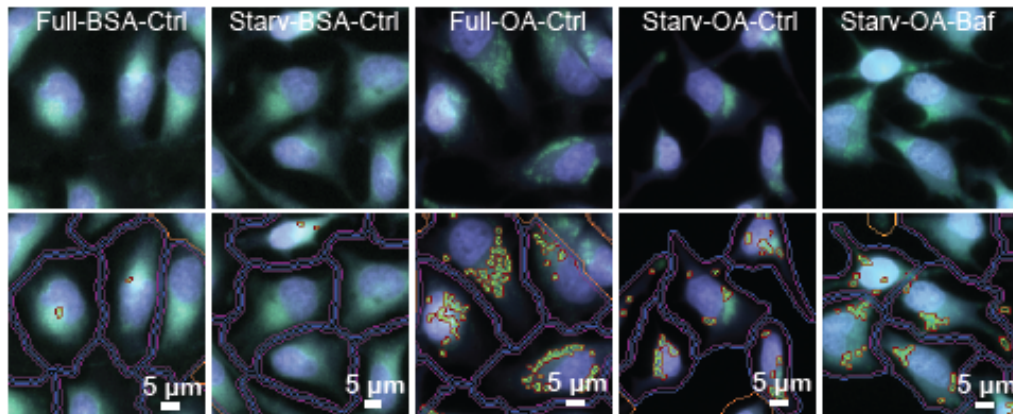


Supplementary Figure S2. Early autophagic markers are recruited to LDs.

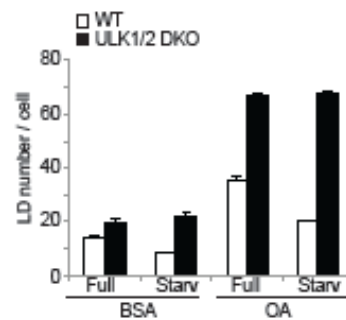
(A-L) Confocal microscopy analysis of U2OS cells stably expressing GFP WIPI-1 (A), GFP WIPI-2B (D), HEK-293 cells stably expressing GFP-DFCP1 (G), and HeLa cells expressing GFP-ATG16L1 (J). Lipid droplets were visualized (blue channel, DROPLET) with LipidTox DeepRed. Cells were pre-treated for 20 h with 500 μM BSA-oleic acid, starved for 1 h (for DFCP1) or 2 h (for WIPIs and ATG16L1) and then analyzed by confocal fluorescence microscopy. Arrowheads, recruitment of WIPIs or DFCP1 or ATG16L1 to lipid droplets. (B,E,H,K) Two-fluorescence channel line tracings corresponding to dashed lines in images to the left. Arrowheads, recruitment of WIPIs, DFCP1, and ATG16L1 to lipid droplets. (C,F,I,L) Quantification of the recruitment of early autophagic markers to LDs. WIPI-1- (C), WIPI-2B- (F), DFCP1- (I) and ATG16L1- (L) positive LDs were quantified by Image J software (details in

Materials and Methods). Cells were pre-treated for 20 h with 500 μ M BSA-oleic acid (OA) then starved (OA Starv) or not (OA Full) for 1 h (for DFCEP1) or 2 h (for WIP1s and ATG16L1) in the absence or presence of 3-MA treatment (OA Starv3MA). Data mean values \pm s.e. ($n \geq 3$); *, $p < 0.05$. (M,N) Subcellular fractionation of membranous organelles in oleic acid-treated cells subjected to starvation (Starv) or not (Ctrl; control). HeLa cells were treated with 200 μ M BSA-oleic acid and then incubated in full medium (A) or starved (B) for 2 h. Cells were then subjected to subcellular fractionation of membranous organelles by isopycnic separation in sucrose density gradients via equilibrium centrifugation. PNS, postnuclear supernatant. Rectangle over fraction 1, convergence in light fractions of early autophagic marker (ATG16L1) with lipid droplets (revealed by ADRP, also known as perilipin 2 or adipophilin). Numbers below lanes, refractive index (reflecting sucrose density) of each fraction. (C,D) Subcellular fractionation of membranous organelles in oleic acid-treated cells subjected to starvation (Starv) or not (Ctrl; control). HeLa cells were treated with 200 μ M BSA-oleic acid and then incubated in full medium (C) or starved (D) for 2 h.

A



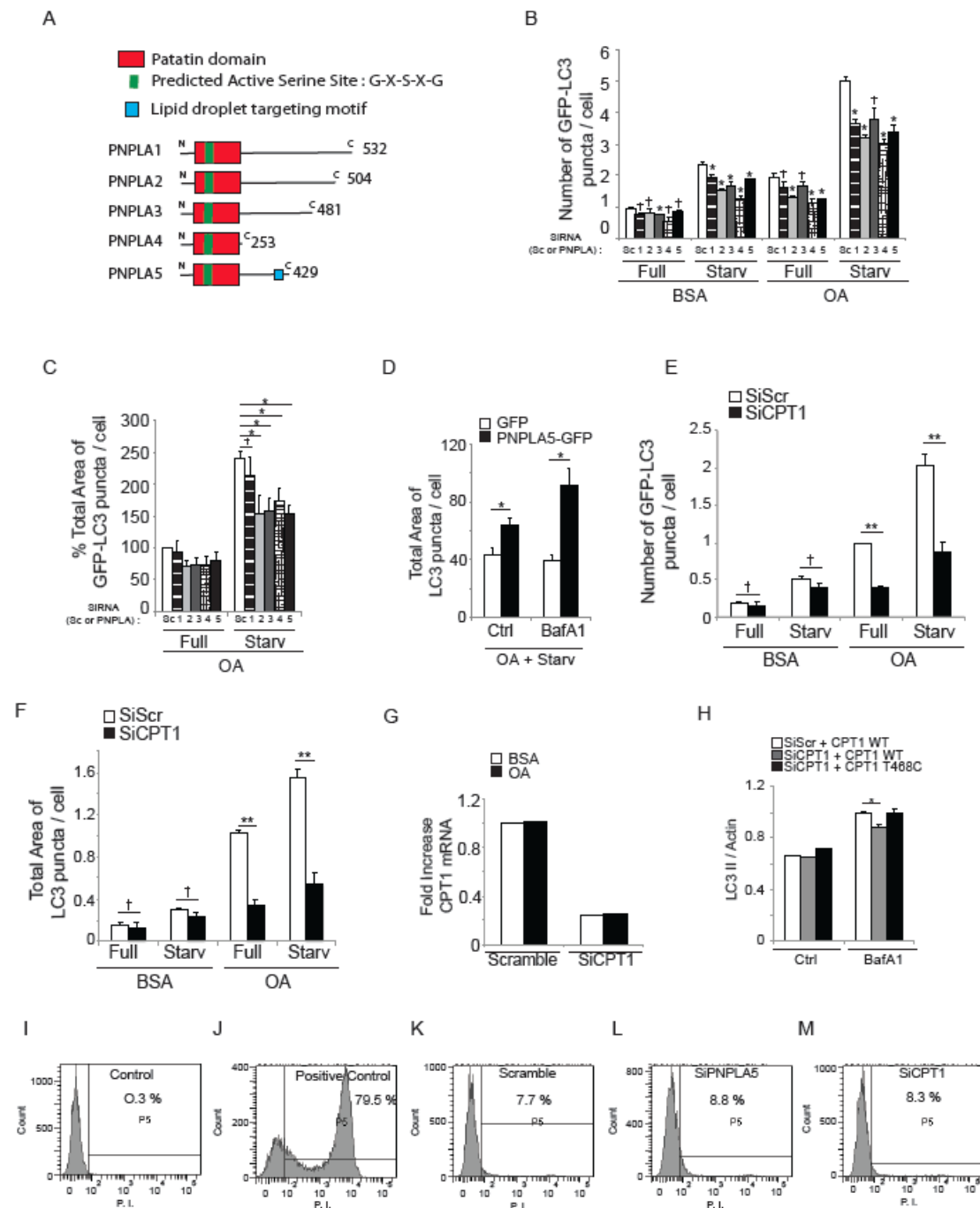
B



Supplementary Figure S3. Effect of Bafilomycin-A1 on lipid droplets degradation upon autophagy induction and change in abundance of lipid droplets upon autophagy induction depends on ULK1 and 2.

(A) Fluorescent images obtained by high content image acquisition and analysis. HeLa cells were treated for 20 h with BSA alone or with 500 μ M BSA-oleic acid (OA) and starved (Starv) or not (Full) for 2 h with or without Bafilomycin A1 (Baf) to inhibit autophagic degradation. Cells were then fixed and nuclei (blue) and lipid droplets (green) were stained for fluorescence microscopy with Hoechst 33342 and Bodipy 493/503 respectively. (B)

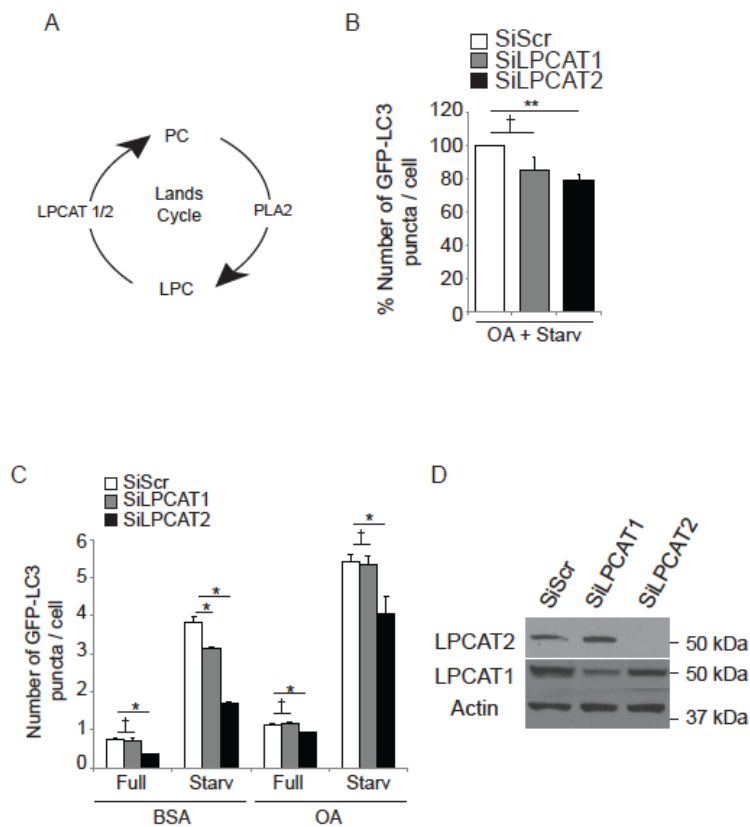
Spontaneously immortalized $Ulk1/2^{+/+}$ (WT) and $Ulk1/2^{-/-}$ (ULK1/2 DKO) murine embryonic fibroblast (MEFs) cells were treated for 20 h with BSA alone or with 500 μ M BSA-oleic acid (OA) and starved (Starv) or not (Full) for 2 h. Cells were then fixed and lipid droplets were stained for fluorescence microscopy with LipidTOX™ DeepRed. LD number per cell were determined by high content image acquisition and analysis.



Supplementary Figure S4. Analysis of triglyceride mobilizing factors PNPLAs and Kennedy biosynthetic cycle in lipid droplet contributions to cellular autophagic capacity.

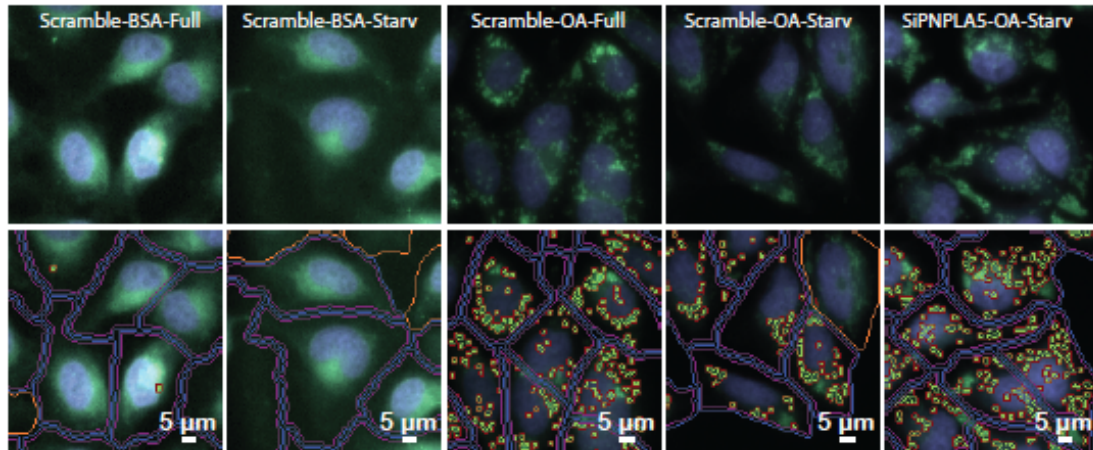
(A) Members of the catalytically active patatin-like phospholipase domain containing proteins, PNPLA1-5. (B,C) Stable mRFP-GFP-LC3 HeLa cells were transfected twice with scramble (Scr) control siRNA or siRNAs against PNPLA1, PNPLA2, PNPLA3, PNPLA4, and PNPLA5. After 24 h following

transfection, cells were treated for 20 h with BSA alone or with 500 μ M BSA-oleic acid (OA) and starved in EBSS or not (full medium) for 90 min. Graph in B, an example of raw data (number of GFP-LC3 dots per cell) from a single high content analysis experiment (data in the main sequence figures include data from 3 or more independent experiments as shown here). Graph in C, total area of GFP+ puncta were quantified by high content image acquisition and analysis. Data represent mean values \pm s.e. ($n \geq 3$); *, $p < 0.05$. (D) Effect of PNPLA5 overexpression on autophagy induction by quantifying total area of endogenous LC3 dots. HeLa cells were transfected either with GFP or PNPLA5-GFP expressing plasmids, then treated 20 h with 500 μ M BSA-OA. Next, cells were starved for 2 h with or without Bafilomycin A1 (Baf). Endogenous LC3 was stained by immunofluorescence and total area of LC3 dots were quantified in GFP-positive cells by high content image acquisition and analysis. Data represent mean values \pm s.e. ($n \geq 3$); *, $p < 0.05$. (E,F) HeLa cells stably expressing mRFP-GFP-LC3 were transfected twice with scrambled (Scr) siRNA or siRNAs against CPT1 (siRNA details are given in Supplementary Table S2). After 24 h post-transfection, cells were treated for 20 h with 500 μ M BSA-OA and starved or not for 90 min. GFP+ puncta per cell were quantified by high content image acquisition and analysis. Data in E, number of GFP+ puncta per cell. Data in F, total area of GFP+ puncta per cell. Data represent mean values \pm s.e. ($n \geq 3$); *, $p < 0.05$. (G) HeLa were transfected twice with control Scr (scramble) siRNA or siRNAs against CPT1. After 48 h following the first transfection, cells were treated 20 h with 500 μ M BSA-OA or with BSA and CPT1 mRNA levels were quantified by real-time RT-PCR and internally normalized with respect to the *Actin* gene. (H) Effect of CPT1 on autophagy induction by measuring LC3-II levels. HeLa cells were transfected with siRNAs against CPT1 or scrambled (Scr) control. After 24 h, cells were cotransfected with siRNAs against CPT1 or scrambled (Scr) control and with plasmids expressing wild-type (WT) CPT1-mCherry or mutant CPT1-mcherry T468C (siRNA resistant construct). Cells were then treated 20 h with 500 μ M BSA-OA and starved for 2 h with or without bafilomycin A1 (Baf) to inhibit autophagic degradation and LC3-II/actin ratios determined by immunoblotting (see Fig. 6L) followed by densitometry. (I-M) Cell viability upon knockdown of PNPLA5 and CPT1. Flow cytometry analysis of propidium iodide (P.I.) positive cells. HeLa cells were transfected twice with scramble (Scr) control siRNA or siRNAs against PNPLA5 or CPT1. After 24 h following transfection, cells were incubated with propidium iodide. As a positive control, cells were fixed with 4% paraformaldehyde for 20 minutes at room temperature before P.I. incubation.



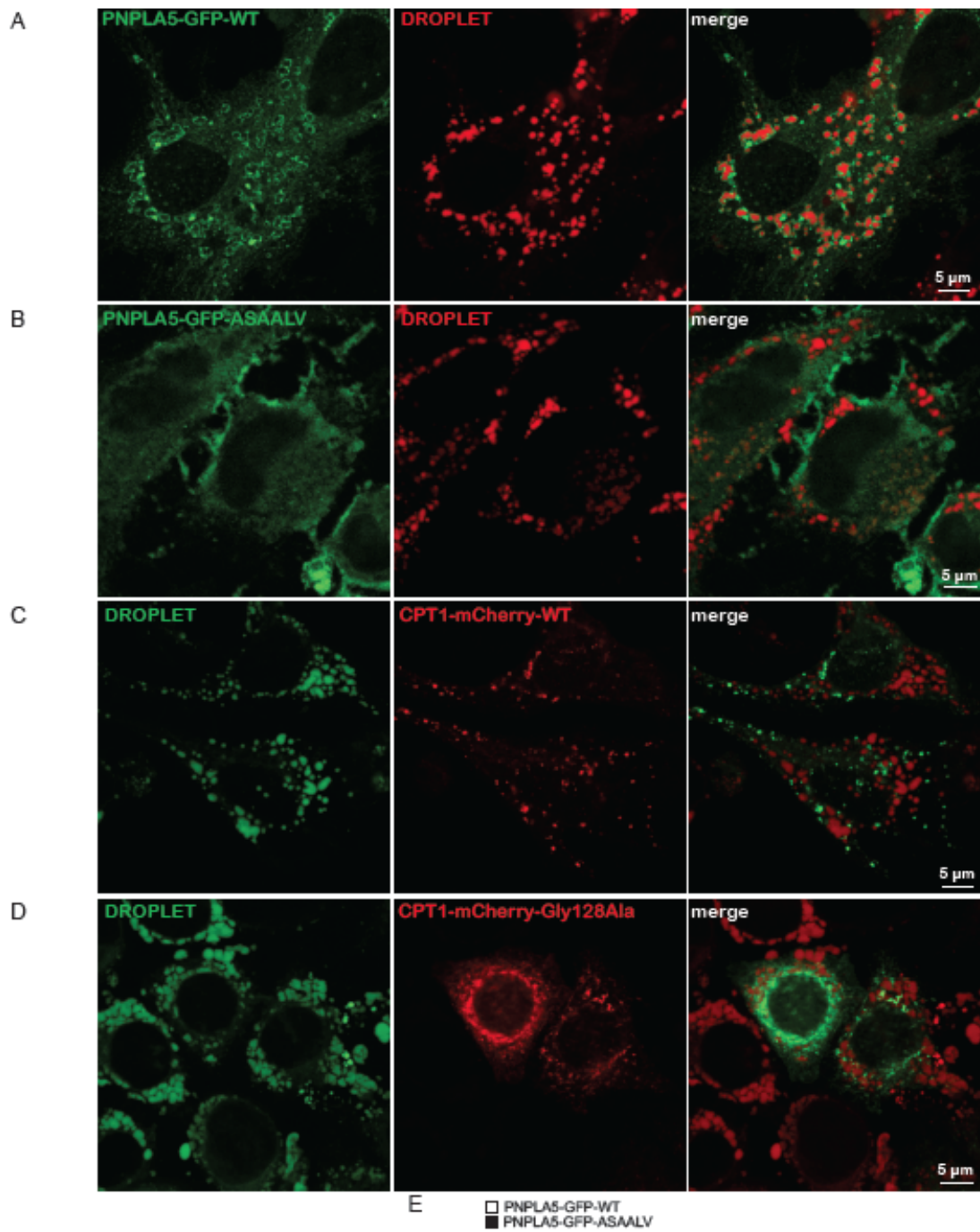
Supplementary Figure S5. Analysis of Lands cycle enzymes in lipid droplet contributions to cellular autophagic capacity.

(A) Schematic, Lands cycle phospholipid remodeling pathway; PLA2, phospholipase A2, LPC, lysophosphatidylcholine; LPCAT, lysophosphatidylcholine acyl-transferase (1 and 2), PC, phosphatidylcholine. (B) HeLa cells stably expressing mRFP-GFP-LC3 were transfected with scrambled control (Scr), LPCAT1, or LPCAT2 siRNAs. 48 h following transfection, cells were treated for 20 h with 500 μ M BSA-oleic acid (OA) and starved or not for 90 min. GFP⁺ puncta per cell were quantified by high content image acquisition and analysis. All high content analysis data, means \pm s.e (n=3, where n represents separate experiments; each experimental point in separate experiments contained >500 cells identified by the program as valid primary objects); *, p<0.05 †, p \geq 0.05 (t-test). (C) HeLa cells stably expressing mRFP-GFP-LC3 were transfected with scrambled (Scr) control siRNA or siRNAs against LPCAT1, LPCAT2 (siRNA details are in Supplementary Table S1). After 48 h of transfection, cells were treated for 20 h with 500 μ M BSA-Oleic Acid (OA) and starved in EBSS or incubated in full medium for 90 min. GFP⁺ puncta per cell were quantified by high content image acquisition and analysis. (D) HeLa cells were transfected with scrambled control siRNA (Scr) or siRNAs against LPCAT1 and LPCAT2. After 48 h of transfection, cells were incubated for 20 h with 500 μ M BSA-Oleic Acid (OA) and LPCAT1 and LPCAT2 levels assayed by immunoblots.



Supplementary Figure S6. Effect of PNPLA5 knockdown on lipid droplets consumption following autophagy induction.

Fluorescent images from high content image acquisition and analysis. HeLa cells were transfected twice with siRNAs PNPLA5 or scramble (Scr) control. Cells were then treated 20 hours with BSA or with 500 μM BSA-Oleic Acid (OA) and starved or not during 2 hours. Cells were then fixed and nuclei (blue) and lipid droplets (green) were stained for fluorescence microscopy with Hoechst 33342 and Bodipy 493/503 respectively.



Supplementary Figure S7. Lipid droplet targeting motif in PNPLA5 is required for its recruitment to LDs and for starvation-induced

consumption of LDs.

Images show confocal microscopy analysis of HeLa cells expressing wild-type (WT) GFP-tagged (A) or ASAALV mutant PNPLA5 proteins (B) or wild-type (WT) mCherry-tagged (C) or CPT1Gly₁₂₈Ala mutant CPT1 (D) proteins. Cells were treated for 20 h with 500 μ M BSA-oleic acid (OA), starved for 2 h, fixed and lipid droplet stained for immunofluorescence with LipidTOX™ DeepRed. (E) HeLa were transfected with plasmids expressing wild-type (WT) GFP-tagged or ASAALV mutant PNPLA5 proteins and treated for 20 h with 500 μ M BSA-oleic acid (OA). Cells were starved for 2 h, fixed and lipid droplets stained for fluorescence microscopy with LipidTOX™ DeepRed. LD numbers per cell were determined by high content image acquisition and analysis.

Supplemental Table

Supplementary Table S1.

Quantification of cytoplasmic LDs [(C)LD], Isolation membrane (IM) and autophagic vacuoles (AV) in electron microscopy pictures (image ID in left column). U2OS cells were treated for 24 h with 500 μ M BSA-oleic acid then fixed and processed for ultrastructure electron microscopy (see Materials and Methods for details).

Image ID	(C)LD	IM	AV	Sum
7575	1	0	0	1
7576	2	1	0	3
7577	10	3	0	13
7578	5	1	0	6
7579	5	0	0	5
7581	5	0	0	5
7582	4	0	0	4
7583	2	0	0	2
7584	1	0	0	1
7588	20	1	0	21
7590	0	1	0	1
7592	1	0	4	5
Sum	56	7	4	67
%	82.54	11.11	6.35	100

Supplemental Experimental Procedures

Antibodies, immunoblotting, detection assays, and conventional microscopy

Blots were analyzed with antibodies to LC3 (Sigma), p62 (BD Transduction), Actin (Sigma), ATG16L1 (Cosmo Bio), Adipophilin (Progen Biotechnik), WIPI2 (Abgent), LPCAT1 (ProteinTech Group Inc), LPCAT2 (Novus Biologicals); staining was revealed with Super Signal West Dura chemiluminescent substrate (Pierce). Immunofluorescence conventional microscopy was carried out with a Zeiss ApoTome 2 piloted with Zen software 2012. Confocal microscopy was carried out using a Zeiss LSM 510 Meta microscope (laser wavelengths 488 nm, 543 nm and 633 nm) or a confocal Leica TCS SP5 (LAS AF version 2.6.0) (laser wavelengths 488 nm, 561 nm and 633 nm). Antibodies against endogenous proteins LC3 (MBL), p62 (BD Transduction), ATG16L1 (Cosmo Bio) were used for indirect immunofluorescence analysis. To preserve lipid droplet structure, immunofluorescence analyses were performed as previously described [S1]. SlideBook morphometric analysis software 5.0 (Intelligent Imaging Innovations) and ImageJ software 1.47n (NIH) were used to quantify the recruitment of early autophagic markers or DAG to lipid droplets. Percentage of ATG16L1 (or WIPI1, WIPI2B, WIPI2D, DFCP1, DAG) positive lipid droplets was fraction of total lipid droplet examined scored as positive when one or more puncta or homogeneously distributed marker were observed overlapping with the mask of lipid droplet (derived from a dilatation at 110% of the area of lipid droplet). Data are from 3 independent experiments in which, each time, more than 300 lipid droplet were analyzed. Pearson's colocalization coefficients between ATG16L and DAG were derived using Slide Book 5.0. Pearson's coefficient was from three independent experiments with five fields per experiment for a total of 15 fields contributing to the cumulative result.

Mutagenesis

To generate mutants of PNPLA5 and CPT1, site-directed mutagenesis was performed using a Quick Change kit (Stratagene), according to the manufacturer's instructions. The sequences of the primers used were as follows: (PNPLA5 RSRALV-F: 5'-CTTCCGCAGCAGAGCGTTGGTGGTGTGGC-3', PNPLA5 RSRALV-R: 5'-GCCACACCACCAACGCTCTGCTGCGGAAG-3', PNPLA5 RSAALV-F: 5'-CTTCCGCAGCGCAGCGTTGGTGGTGTGGCTGCCCG-3', PNPLA5 RSAALV-R: 5'-CGGGCAGCCACACCACCAACGCTGCGCTGCGGAAG-3', PNPLA5 ASAALV-F: 5'-GTACATCTACTTCGCCAGCGCAGCGTTGGTGG-3', PNPLA5 ASAALV-R: 5'-CCACCAACGCTGCGCTGGCGAAGTAGATGTAC-3') for PNPLA5 LTM (lipid droplet targeting) mutant; (CPT1 Gly128Ala-F: 5'-CTCTTGTCCCTTTAGCGGAGCTCTTTGACCATG-3', CPT1 Gly128Ala - R: 5'-CATGGTCAAAGAGCTCCGCTAAAGGGGAACAAGAG-3') for CPT1 mutant on the catalytic site; (CPT1 T468C-F: 5'-AACCAGTCAGGGTAAGTTCCTAAGCGAGCGGCA-3', CPT1 T468C-R: 5'-

TGCCGCTCGCTTAGGAACTTACCCTGACTGGTT-3') for CPT1 siRNA resistant experiment.

Proteolysis of stable proteins

Two proteolysis assays were used: (i) bafilomycin A1-dependent degradation of the whole bulk of proteins (ii) degradation of long-lived proteins. For assay (i), proteins from HeLa cells were radiolabeled by incubation in complete medium containing oleic acid and 0.2 $\mu\text{Ci/ml}$ of L- ^{14}C valine. Following 20 h of radiolabeling, cells were incubated with fresh complete medium containing 10 mM cold valine for 1 h to degrade short-lived proteins. After this period, the medium was removed and replaced with the appropriate fresh complete medium supplemented with 10 mM cold valine, and incubated for further 4 hours. To stimulate autophagy, EBSS containing 10 mM cold valine and 0,1% of bovine serum albumin were used. For assay (ii), proteins from HeLa cells were radiolabeled by incubation in complete medium containing oleic acid and 1 $\mu\text{Ci/ml}$ [^3H] leucine. Following 20 h of radiolabeling, cells were incubated in full or starvation media with or without bafilomycin A1 for 90 min. For both assays, trichloroacetic acid (TCA)-precipitable radioactivity in the cells and the TCA-soluble radioactivity released into the media were determined. Leucine or valine release (a measure of proteolysis) was calculated as a ratio between TCA-soluble supernatant and total cell-associated radioactivity.

Mycobacterial survival

Microbiological analyses of bacterial viability (*M. bovis* BCG) were carried out as previously described [S2].

Knockdowns with siRNAs and knockdown validation

HeLa, NIH3T3 and RAW 264.7 cells were transfected by nucleoporation using Nucleofector Reagent Kit R, V and V (Amaxa/Lonza biosystems) or by using the FUGENE 6 HD transfection reagent (Promega) or Lipofectamine 2000 (Invitrogen) according to the manufacturer's instructions. Non-targeting siRNA pool (Scrambled) was used as a control. Knockdown validation was carried out either by immunoblotting or quantitative RT-PCR. SMARTpool SiGENOME siRNAs from Dharmacon-Thermoscientific used in this study were as follows: (human PNPLA1: M-009042-00-0005, human PNPLA2: M-009003-01-0005, human PNPLA3: M-009564-01-0005, human PNPLA4 : M-010271-01-0005, human PNPLA5: M-009563-01-0005, human CHPT1 (CPT1): M-009775-02-0005, mouse PNPLA5: M-048942-01-0005, control: D-001206-13-20). Non-Smartpool siRNA used for siRNA-resistant experiments is : human CHPT1 (CPT1), D-009775-01-0005.

Quantitative RT-PCR

Total RNA was extracted from cells and cDNA was synthesized using a Cells-to-Ct Kit (Applied Biosystems), according to the manufacturer's instructions. Real time PCR was performed using SYBR Green Master Mix (Applied Biosystems), and products were detected on a Prism 5300 detection system (SDS, ABI/Perkin-Elmer). The relative extent of PNPLA1, PNPLA2, PNPLA3, PNPLA4, PNPLA5, CPT1 expression was calculated using the $2^{-\Delta\Delta C(t)}$ method. Conditions for real time PCR were: initial denaturation for 10 min at 95°C, followed by amplification cycles with 15 sec at 95°C and 1 min at 60°C.

RT-PCR human primers used for knockdown validation were as follows:
(Actin-F: 5'-AAGACCTGTACGCCAACACA-3', Actin-R: 5'-TGATCTCCTTCTGCATCCTG-3', PNPLA1-F: 5'-CCAGATAGAACTCGCCCTTG-3', PNPLA1-R: GTGAGGTTGTGTGGCTCCTT, PNPLA2-F: CAACACCAGCATCCAGTTCA, PNPLA2-R: ATCCCTGCTTGCACATCTCT, PNPLA3-F: ATGTCCACCAGCTCATCTCC, PNPLA3-R: GCATCCACGACTTCGTCTTT, PNPLA4-F: AGAACCGACTGCACGTATCC, PNPLA4-R: TGCTGGCTAGGAGGACCTTA, PNPLA5-F: TCCTGGGGCTCATATGTCTC, PNPLA5-R: AGTCCACGTCTCTCCAGGAA, CPT1-F: CACCGAAGAGGCACCATACT, CPT1-R, CTTCTGGCTTGTTTCCCATC)

Subcellular fractionation

Subcellular membranous organelles were separated by isopycnic centrifugation in sucrose gradients as described [S3]. Cells were homogenized in 250 mM sucrose, 20 mM HEPES-NaOH pH 7.5, 0.5 mM EGTA, post nuclear supernatant layered atop of pre-formed 60 - 15% sucrose gradients, and samples centrifuged at 100,000 g in a Beckman SW 40 rotor for 18 h at 4 °C. Equivalent density fractions (verified for refractive index match) were analyzed by immunoblotting.

Mitotracker staining and flow cytometry

HeLa cells were stained with 300 nM of mitotracker Green (Molecular Probes) during 15 minutes at 37°C. Flow cytometry was carried out on the LSR Fortessa (BD Biosciences) and data analyzed using FlowJo software (TreeStar).

Propidium iodide staining and flow cytometry

HeLa cells were stained with 1 µg/ml of propidium iodide (Sigma) during 5 minutes at RT. Flow cytometry was carried out on the LSR Fortessa (BD Biosciences) and data analyzed using Diva software.

High content image acquisition and analysis

Two different automated high content analysis system ((Cellomics Array Scan, Thermo Scientific) and (Opera QEHS, Perkin Elmer)) were used to acquire images by computer-driven (operator independent) collection of 49 valid fields per well with cells in 96 well plates, with >500 cells (identified by the program as valid primary object) per each sample. Objects were morphometrically and statistically analyzed using the iDev software (for pictures acquired with Cellomics, Thermo Scientific) or the Acapella software (for pictures acquired with Opera, Perkin Elmer). Computer-driven identification of primary and secondary objects was based on predetermined parameters, and fluorescent objects (cells, puncta, droplets, total cytoplasm) were quantified using a suite of applicable parameter (including number of objects per cell; total area per cell; total intensity). Briefly, nuclei and its associated cytoplasm were sequentially segmented using the Hoechst channel, GFP fluorescent puncta or endogenous LC3 and p62 were revealed by fluorescent antibody staining. Bodipy 493/503, LipidTOX™ Red and LipidTOX™ DeepRed (Molecular Probes) were used to stain lipid droplets.

Time-lapse imaging of cultured cells

Oleic acid-pretreated HeLa cells expressing GFP-LC3 or GFP-DAG or GFP-WIPI-2D were labeled with LipidToxFarred (red) during 5 minutes at RT. Cells were starved and imaged by confocal microscopy. Live-cell fluorescence imaging was performed with an inverted microscope (confocal TCS SP5, Leica, LAS AF version 2.6.0), a 63x PlanAPO oil-immersion objective lens (NA 1.4). Two-color time-lapse images were acquired with appropriate exposure times at 340 ms intervals.

Electron microscopy

U2OS cells were treated with 500 μ M oleic acid for 24 h and fixed in 3.7% paraformaldehyde for 20 min at room temperature. The cell monolayers were collected and further fixed in 2% glutaraldehyde and 0.5% osmium tetroxide in 0.1x PBS, dehydrated with ethanol, and embedded in Epon using standard procedures as previously described [S4]. Thin sections were cut using an ultramicrotome, contrasted with uranyl acetate and lead citrate, examined in an EM410 electron microscope (Philips), and images documented digitally (Ditabis).

Intravital imaging

All experiments were approved by the National Institute of Dental and Craniofacial Research (NIDCR, National Institute of Health, Bethesda, MD, USA) Animal Care and Use Committee. GFP-LC3 mice [S5] were fed ad libitum prior to the procedure. The animals were anesthetized with a mixture of ketamine and xylazine as described [S6]. The liver was exposed by performing a transversal incision (1 cm x 1 cm) in the right side of the abdomen just below the diaphragm. The exposed organ was bathed for 30 minutes with Bodipy 665 positioned on the pre-warmed stage of an Olympus Fluoview 1000 [6]. The temperature of the body and the organ were continuously monitored and maintained with a heat lamp. Time lapse-imaging was performed by confocal microscopy (Excitation for GFP: 488 nm; Excitation for Bodipy 665: 561 nm), as previously described [S6].

Supplemental References

- S1. Listenberger, L.L., and Brown, D.A. (2007). Fluorescent detection of lipid droplets and associated proteins. *Current protocols in cell biology /* editorial board, Juan S. Bonifacino ... [et al.] *Chapter 24*, Unit 24 22.
- S2. Ponpuak, M., Davis, A.S., Roberts, E.A., Delgado, M.A., Dinkins, C., Zhao, Z., Virgin, H.W.t., Kyei, G.B., Johansen, T., Vergne, I., et al. (2010). Delivery of cytosolic components by autophagic adaptor protein p62 endows autophagosomes with unique antimicrobial properties. *Immunity* 32, 329-341.
- S3. Singh, S.B., Ornatowski, W., Vergne, I., Naylor, J., Delgado, M., Roberts, E., Ponpuak, M., Master, S., Pilli, M., White, E., et al. (2010). Human IRGM regulates autophagy and cell-autonomous immunity functions through mitochondria. *Nat Cell Biol* 12, 1154-1165.
- S4. Robenek, H., Robenek, M.J., Buers, I., Lorkowski, S., Hofnagel, O., Troyer, D., and Severs, N.J. (2005). Lipid droplets gain PAT family

proteins by interaction with specialized plasma membrane domains. *J Biol Chem* **280**, 26330-26338.

- S5. Mizushima, N., Yamamoto, A., Matsui, M., Yoshimori, T., and Ohsumi, Y. (2004). In vivo analysis of autophagy in response to nutrient starvation using transgenic mice expressing a fluorescent autophagosome marker. *Mol Biol Cell* **15**, 1101-1111.
- S6. Masedunskas, A., Sramkova, M., Parente, L., Sales, K.U., Amornphimoltham, P., Bugge, T.H., and Weigert, R. (2011). Role for the actomyosin complex in regulated exocytosis revealed by intravital microscopy. *Proceedings of the National Academy of Sciences of the United States of America* **108**, 13552-13557.